Arbitrary Sampling Rate Conversion of Complex Signals

Gennaro Evangelista[1], *Heinz G. Göckler*[2],
[1]Siemens ICM, Munich, Germany,
[2]Digital Signal Processing Group, Ruhr-Universität Bochum, Germany.
email: gennaro.evangelista@mch.siemens.de

ABSTRACT

The conversion of complex-valued digital signals from a given sampling rate to a second, arbitrary sampling rate, with both sampling rates derived from independent clock generators, is investigated for the first time. Different efficient systems are presented and compared concerning the required computational burden.

1 Introduction

The need of sample rate conversion is omnipresent in the world of digital signal processing: 1. Choosing the lowest possible sampling rate in compliance with the sampling theorem in order to minimise the overall computational burden of a digital system 2. Independent specification of sampling and data rates in communications systems for digital audio and image processing, software radio and digital receivers, etc. In the latter case, digital subsystems operated at asynchronous sampling rates that are derived from independent clock generators have to be matched by an Arbitrary Sampling Rate Converter (ASRC).

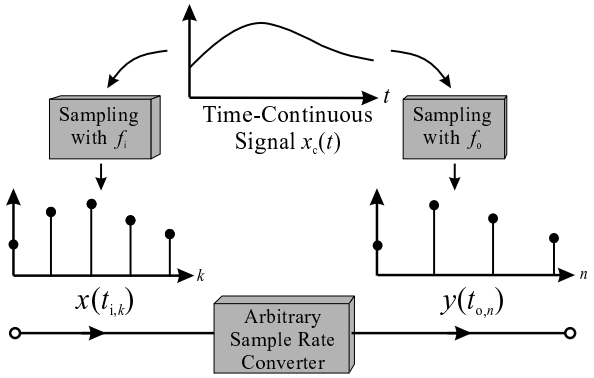

Figure 1: Model of arbitrary sampling rate conversion

The model approach to ASRC is depicted in Fig. 1 for real input and output signals, where $f_\mathrm{i} = 1/T_\mathrm{i}$ and f_o represent the input and output sampling rates, respectively: The equidistantly sampled digital input signal $x(t_{\mathrm{i},k}) = x(kT_\mathrm{i}) = x_\mathrm{c}(t)|_{t=kT_\mathrm{i}}$ is conceptually interpolated to yield an intermediate (fictive) time-continuous signal for subsequent resampling: $y(t_{\mathrm{o},n}) = x_\mathrm{c}(t)|_{t=t_{o,n}}$, where the output sampling rate f_o may be slowly time-varying.

In the past, ASRC of real-valued signals has thoroughly been studied [1-4,6]. It is the goal of this contribution to apply those results to complex-valued signals since, for instance, modern digital communications systems are commonly based on the processing of complex signals.

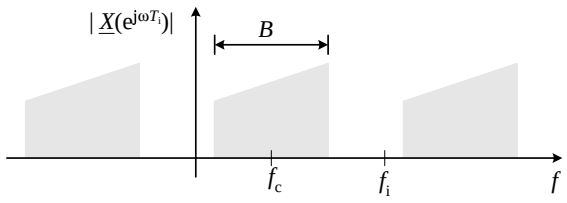

Figure 2: Spectrum of a general complex digital signal $\underline{x}(kT_\mathrm{i})$ for $f_\mathrm{i} > B > \frac{f_\mathrm{i}}{2}$; $\omega = 2\pi f$

The spectrum of a general complex-valued digital signal $\underline{x}(kT_\mathrm{i}) = x_\mathrm{R}(kT_\mathrm{i}) + \mathrm{j}x_\mathrm{I}(kT_\mathrm{i})$ of bandwidth B and centre frequency f_c is shown in Fig. 2, where underlining is used to distinguish complex from real (time-domain) signals. Reasonable oversampling (by a factor of less than 2) is assumed.

In section 2 the most efficient implementation of ASRC for real signals is recalled [1, 6]. Next, this ASRC system is used to develop a variety of novel approaches to ASRC of complex signals. Finally, the presented methods are discussed and compared.

2 Efficient Implementation of Real ASRC

The general and highly flexible approach to ASRC of real-valued signals (RASRC) is depicted in Fig. 3 [1, 4, 6]. Upsampling by L in conjunction with lowpass filtering $h(\nu\frac{T_\mathrm{i}}{L})$ realises integer (L-synchronous) sample rate conversion (ISRC). The subsystem with impulse re-

sponse $g(t)$ and subsequent output sampling at f_o represents the quasi-continuous approximation. Here, each RASRC output sample $y(t_{o,n})$ is derived from a subset of η contiguous values $u(\nu\frac{T_i}{L})$ taken from successive blocks of L output samples of ISRC.

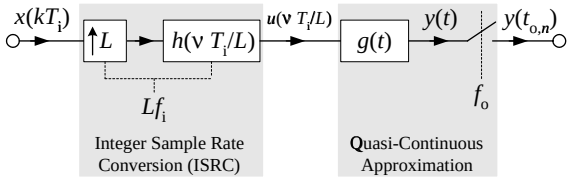

Figure 3: General approach to real ASRC

The most efficient implementation of RASRC [1] deduced from Fig. 3 is shown in Fig. 4 with $h(\nu\frac{T_i}{L})$ as an FIR filter. It applies polyphase (PP) decomposition for ISRC [5] with low-rate branch filtering at f_i:

$$h_\lambda(\nu T_i) = h([\nu L + \lambda]\tfrac{T_i}{L}), \quad \lambda = 0, \ldots, L-1, \qquad (1)$$

and the FARROW-structure (FS) [2] for quasi-continuous (ζ -1)-order polynomial approximation. The choice of the respective η output samples of ISRC is governed by the actually prescribed sampling instant $t_{o,n}$ of the RASRC output signal. As a result, for each output sample $y(t_{o,n})$ only η out of L PP branch filters (1) of the ISRC must be activated at a time.

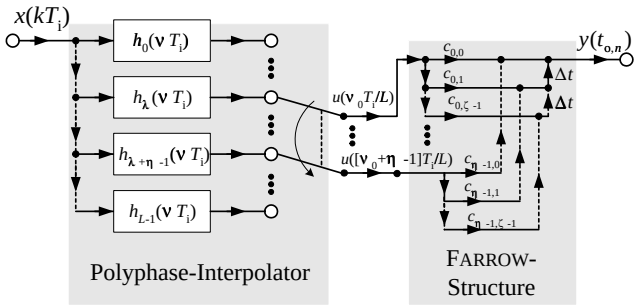

Figure 4: Efficient realisation of RASRC; $\nu_0 = \lfloor \frac{t_{o,n}}{T_i/L} \rfloor$, $\Delta t = \frac{t_{o,n}}{T_i/L} - \nu_0$

3 ASRC of Complex Signals

The spectrum of the complex signal $\underline{x}(kT_i)$ to be converted is depicted in Fig. 2 for arbitrary f_c. As a coarse yet suitable measure of the computational burden the multiplication rate M, the number of real-valued multiplications times the respective sampling rate, is adopted. The cases $f_c \approx \{0, f_i/2\}$ are self-evidently implied in most of the ASRC approaches to be presented.

3.1 Complex ASRC System

ASRC of a complex signal as defined by Fig. 2 calls for complex parameters of both the PP-interpolator and, potentially, the FS, as shown in Fig. 4. Note that, in compliance with Figs. 3 and 4, all multiplications of the PP-interpolator are carried out at f_i, whereas the FS completely operates at f_o.

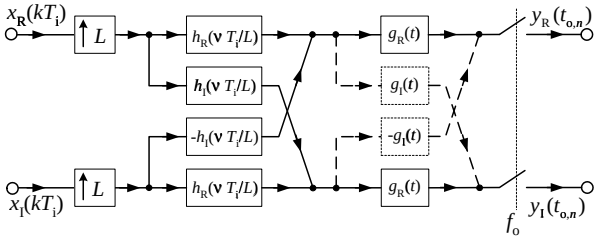

Figure 5: Complex ASRC with complex $\underline{h}(\nu\frac{T_i}{L})$ and a) complex $\underline{g}(t)$ (CASRC1 with dashed blocks), b) real $g(t)$ (CASRC2 without dashed blocks)

First the PP interpolator is considered. The relative transition bandwidth of $\underline{H}(e^{j\omega T_i/L})$ is evidenced from Fig. 6: $\frac{f_i - B}{L f_i}$. As a result, the multiplication rate of ISRC is given by: $\frac{4aLf_i^2}{f_i - B}\frac{\eta}{L}$, where a represents a constant factor depending on the filter specifications [5] and η the number of active PP branch filters (cf. Fig. 4). A widespread approach to the design of complex FIR filters applies modulation:

$$\underline{h}(\nu\tfrac{T_i}{L}) = h(\nu\tfrac{T_i}{L})e^{j2\pi f_c T_i \nu/L}. \qquad (2)$$

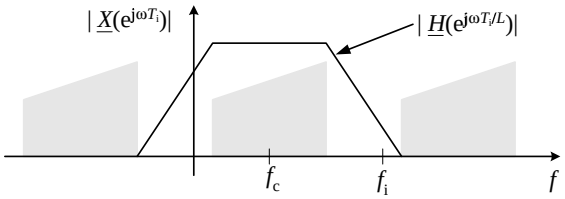

Figure 6: Specification of $\underline{h}(\nu\frac{T_i}{L})$ for CASRC1-3

Next, three options of quasi-continuous approximation are examined. The first straightforward approach (CASRC1) calls for a complex $\underline{g}(t)$, as shown in Figs. 5 and 7, and thus, for a complex (modified) FS. In case of great L, a real FS (CASRC2) requires roughly the same order for $g(t)$ (cf. Figs. 5 and 7). The third option (CASRC3), depicted in Fig. 8, shifts the signal spectrum to zero centre frequency for $g(t)$ filtering.

For CASRC1 the impulse response $\underline{g}(t)$ of the complex FS is again derived by the frequency shifting approach according to (2), which yields complex coefficients $\underline{c}_{\mu,\nu}$, real time-varying sampling instants Δt and

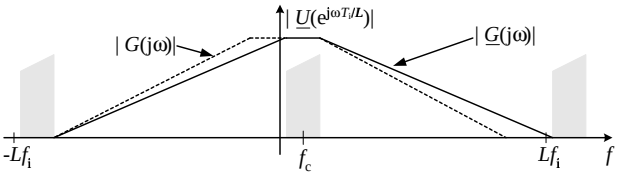

Figure 7: Specification of complex $\underline{g}(t)$ (solid), real $g(t)$ (dashed)

an additional mixer $e^{j2\pi f_c T_i \Delta t/L}$ at the output of the complex FS. Hence, for computation of each complex output sample, the complex FS requires $4\eta\zeta$ real multiplications for $\underline{c}_{\mu,\nu}$, $2(\zeta-1)$ for Δt and 4 for $e^{j2\pi f_c T_i \Delta t/L}$. A tentative approach (which still calls for verification) subsequently applies the dependency of FIR expenditure on the frequency response transition band [5] also to quasi-continuous approximation. As a result, the overall CASRC1-multiplication rate is given by

$$M_{\mathrm{CASRC1}} = \frac{4a\eta}{1-B/f_\mathrm{i}} f_\mathrm{i} + \frac{2b(2\eta\zeta+\zeta-1)}{1-B/Lf_\mathrm{i}} f_\mathrm{o} + 4f_\mathrm{o} \quad (3)$$

with a and b being suitable constant factors.

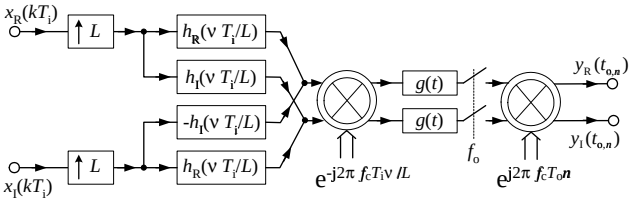

Figure 8: CASRC3 with complex $\underline{h}(\nu\frac{T_\mathrm{i}}{L})$ and real $g(t)$

For CASRC2 with real FS, the relative width of the CASRC1-transition band of $G(\mathrm{j}\omega)$ is reduced by the amount of $\frac{2f_\mathrm{c}}{Lf_\mathrm{i}}$ to $(1-\frac{B+2f_\mathrm{c}}{Lf_\mathrm{i}})$, as it can be deduced from Fig. 7. Hence, the overall CASRC2-multiplication rate is given by

$$M_{\mathrm{CASRC2}} = \frac{4a\eta}{1-B/f_\mathrm{i}} f_\mathrm{i} + \frac{2b(\eta\zeta+\zeta-1)}{1-B/Lf_\mathrm{i}-2f_\mathrm{c}/Lf_\mathrm{i}} f_\mathrm{o}. \quad (4)$$

Finally, the expenditure of the CASRC3-approach according to Fig. 8 is easily obtained by considering that *i*) the transition band of $G(\mathrm{j}\omega)$ is identical to that of CASRC1, *ii*) the first mixer has to perform η complex multiplications at f_i (cf. Fig. 4), and *iii*) the output mixer carries out just one complex multiplication at f_o. Hence, the CASRC3-multiplication rate is given by

$$M_{\mathrm{CASRC3}} = \frac{4a\eta}{1-B/f_\mathrm{i}} f_\mathrm{i} + 4\eta f_\mathrm{i} + \frac{2b(\eta\zeta+\zeta-1)}{1-B/Lf_\mathrm{i}} f_\mathrm{o} + 4f_\mathrm{o}. \quad (5)$$

3.2 Real-Valued ASRC System

Subsequently, ASRC of complex signals according to Fig. 2 is to be performed by a completely real-valued ASRC system (RASRC). This is achieved by suitable pre- and postprocessing.

3.2.1 Modulation Approach (MASRC)

Moving the inner frequency translation of CASRC3 directly to the system input leads to the modulation approach (MASRC), as it is depicted in Fig. 9 with ISRC as an PP interpolator. Since CASRC3 and MASRC rely on the same (merely frequency shifted) specification, the overall multiplication rate is immediately obtained by adapting (5) correspondingly:

$$M_{\mathrm{MASRC}} = 4f_\mathrm{i} + \frac{2a\eta}{1-B/f_\mathrm{i}} f_\mathrm{i} + \frac{2b(2\eta\zeta+\zeta-1)}{1-B/Lf_\mathrm{i}} f_\mathrm{o} + 4f_\mathrm{o}. \quad (6)$$

The associated spectra and filter transfer functions are easily deduced from Figs. 6 and 7.

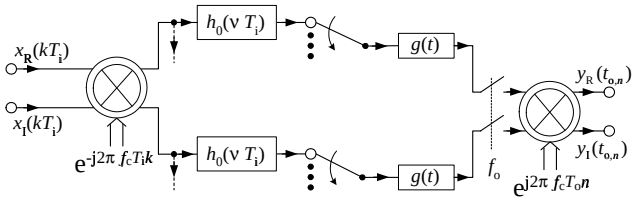

Figure 9: Modulation approach (MASRC)

3.2.2 Analytic Signal Processing Approach (AASRC)

The analytic signal processing approach (AASRC), depicted in Fig. 10, first transforms the complex input signal $\underline{x}(kt_\mathrm{i})$ into the associated analytic signal with twice the sample rate by means of the filter $\underline{P}(e^{j\omega T_\mathrm{i}/2})$, as shown in Fig. 11 a). This approach to preprocessing is obviously restricted to $f_\mathrm{c} > \frac{B}{2}$. RASRC is applied to the real part of the analytic signal, $x'(k\frac{T_\mathrm{i}}{2})$, to yield the real output signal $y'(n\frac{T_\mathrm{o}}{2})$ according to the spectral representation Fig. 11 b). Finally the real signal $y'(n\frac{T_\mathrm{o}}{2})$ is extended to a complex signal $\underline{y}(nT_\mathrm{o})$ by the HILBERT filter $\underline{Q}(e^{j\omega T_\mathrm{o}/2})$ decimating by two (cf. Fig. 11 c).

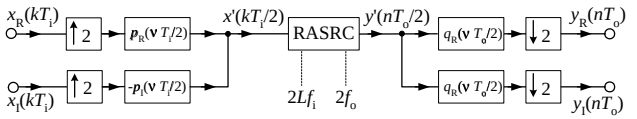

Figure 10: Analytic signal processing approach

Considering that the RASRC is operating at $2f_\mathrm{i}$ and $2f_\mathrm{o}$ and that $\underline{p}(\nu\frac{T_\mathrm{i}}{2})$ and $\underline{q}(\nu\frac{T_\mathrm{o}}{2})$ are realised as PP interpolator and decimator, the AASRC-multiplication rate is given by:

$$\begin{aligned} M_{\mathrm{AASRC}} &= \frac{4a_p}{1-B/f_\mathrm{i}} f_\mathrm{i} + \frac{2a\eta}{1-B/2f_\mathrm{i}-f_\mathrm{c}/f_\mathrm{i}} f_\mathrm{i} \\ &\quad + \frac{2b(\eta\zeta+\zeta-1)}{1-B/2Lf_\mathrm{i}-f_\mathrm{c}/Lf_\mathrm{i}} f_\mathrm{o} + \frac{4a_q f_\mathrm{o}^2}{2f_\mathrm{c}-B}, \quad (7) \end{aligned}$$

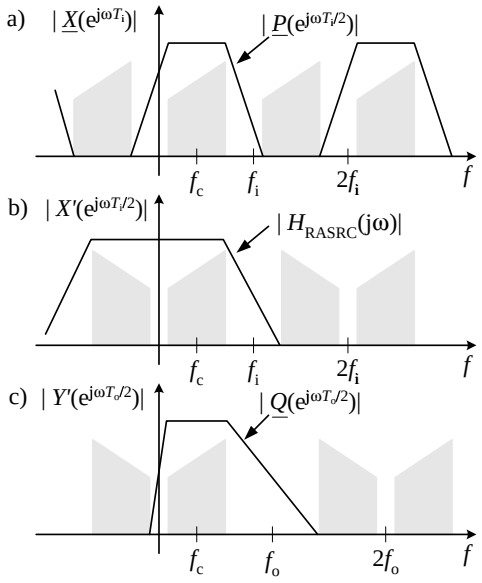

Figure 11: Specification of a) $\underline{P}(\mathrm{e}^{\mathrm{j}\omega T_\mathrm{i}/2})$, b) RASRC, c) $\underline{Q}(\mathrm{e}^{\mathrm{j}\omega T_\mathrm{o}/2})$

where the relative transition bandwidths of $\underline{P}(\mathrm{e}^{\mathrm{j}\omega T_\mathrm{i}/2})$, $\underline{Q}(\mathrm{e}^{\mathrm{j}\omega T_\mathrm{o}/2})$, $H(\mathrm{e}^{\mathrm{j}\omega T_\mathrm{i}/2L})$ and $G(\mathrm{j}\omega)$ can be deduced from Fig. 11.

3.3 Comparison

The relative cost of the described approaches to ASRC of complex signals is compared by means of the multiplication rates (3)-(7). For the set of parameters $\frac{f_\mathrm{c}}{f_\mathrm{i}} = 0.45$, $\frac{B}{f_\mathrm{i}} = 0.8$, $L = 10$, $\eta = \zeta = 2$ and all constants $a \approx b \approx a_p \approx a_q \approx 1$, the relative multiplication rates M/f_i are plotted in Fig. 12 against the sample rate conversion ratio $f_\mathrm{o}/f_\mathrm{i}$.

For nearly all tested sets of parameters MASRC requires the least compuation followed by CASRC2. In case of great L and great $f_\mathrm{o}/f_\mathrm{i}$ CASRC2 is slightly more efficient than MASRC since *i*) MASRC needs additional multiplications by $e^{-\mathrm{j}2\pi f_\mathrm{c} T_\mathrm{i} \nu}$ and $e^{\mathrm{j}2\pi f_\mathrm{c} T_\mathrm{o} n}$ and *ii*) the difference of the relative transition bandwidths of $G(\mathrm{j}\omega)$ becomes negligible.

CASRC1/3 compare badly with the above optimal approaches: CASRC1 because of the complex-valued FS, CASRC3 because of the multipliers $e^{-\mathrm{j}2\pi f_\mathrm{c} T_\mathrm{i} \nu / L}$ and $e^{\mathrm{j}2\pi f_\mathrm{c} T_\mathrm{o} n}$.

AASRC always requires the highest expenditure due to pre- and postfiltering and the operation of RASRC at twice the sampling rates, $2f_\mathrm{i}$ and $2f_\mathrm{o}$, respectively. Note that the increased passband deviation caused by pre- and postfiltering has neither been considered nor compensated by higher filter orders in this comparison. However, AASRC is extremely sensitive to $\frac{f_\mathrm{c}}{f_\mathrm{i}}$ and $\frac{B}{f_\mathrm{i}}$ (cf. Fig. 11). As a result for some system specifications and by the application of half band filters [5] for pre- and postfiltering the gap of the multiplication rates will be considerably smaller.

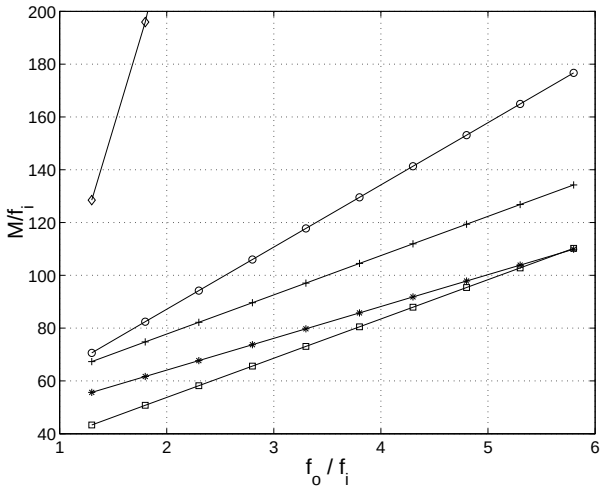

Figure 12: Multiplication rates M/f_i of CASRC1 ($\circ$), CASRC2 ($*$), CASRC3 ($+$), MASRC ($\square$), AASRC ($\diamond$)

4 Conclusion

Arbitrary sampling rate conversion of complex signals has been investigated for the first time. With MASRC and CASRC2 two efficient methods have been presented. However, it depends on the set of parameters $\{L, \eta, \zeta, \frac{B}{f_\mathrm{i}}, \frac{f_\mathrm{c}}{f_\mathrm{i}}\}$ which of these approaches outperforms the other.

References

[1] G. Evangelista, *Zum Entwurf digitaler Systeme zur asynchronen Abtastratenumsetzung*, Ph.D. Thesis, Ruhr-Universität Bochum, December 2000.

[2] C. W. Farrow, *A Continuously Variable Digital Delay Element*, ISCAS'88, Helsinki, Finland, 3:2641-2645, June 1988.

[3] R. Lagadec, D. Pelloni, D. Weiss, *A 2-Channel, 16-bit Digital Sampling Frequency Converter for Professional Digital Audio*, ICASSP'82, 1:93-96, Paris, France, May 1982.

[4] T. A. Ramstad, *Digital Approaches for Conversion Between Arbitrary-Sampling Frequencies*, IEEE Trans. on Acoustics, Speech, Signal Processing, ASSP-3:577-591, June 1984.

[5] P. P. Vaidyanathan, *Multirate Systems and Filter Banks*, Englewood Cliffs: Prentice Hall, 1993.

[6] J. Vesma, *Optimization and Applications of Polynomial-Based Interpolation Filters*, Ph.D. Thesis, Tampere University of Technology, 1999.